P-22

Fully Self-Consistent Calculation the Large-Signal Response of a Double-Barrier Heterostructure Device

Wan-Rone Liou[1] and Mei-Ling Yeh[2]

[1] Department of Electrical Engineering,
National Taiwan Ocean University, Keelung, Taiwan, R.O.C.
TEL: +886-24622192 Ext 6234 FAX: +886-24622192 Ext 6203

[2] Department of Electronics, Nan-Tai Junior College of Technology and Commerce, Tainan, Taiwan, R.O.C.

ABSTRACT

A fully self-consistent large-signal double-barrier (DB) heterostructure model is reported in this paper. Both dc and ac potentials are self-consistently solved with the Poisson and Schrödinger equations. This ensures that the model provides consistent topologies for both current and charge conservation of each harmonic. With this approach we can really count the impact of ac charge on the harmonic current calculation. Harmonic balance based simulation technique is used to calculated the frequency properties of primary harmonic as well as higher harmonics. A conventional undoped AlGaAs/GaAs/AlGaAs DB structure with thickness of 34Å/34Å/34Å sandwiched between two lightly doped GaAs spacers is used as a test device. Generalized Wannier Picture is used to analyze this DB structure. In this paper, we also develop a new wave function matching technique to estimate the Hamiltonian elements at the interfaces of heterostructure.

Fig. 1 and 2 display the impact of charge variation inside the quantum well on the ac potential. Obviously, it is very important to include the ac part into the self-consistent calculation loop if we want to gain more accurate results. A percent error of 0.1 for both dc and ac parts requires about 10 interations outside the NDR region and 20 to 30 interations in the NDR region. Since nonlinearities inherent with DB heterostructures may cause severe degradation in the performance of oscillation circuits, the degree of total harmonic distortion in negative differential resistance (NDR) region for different signal level and frequency is therefore invested in Fig. 3 and Fig 4. Fig. 5 displays the first four harmonic currents as function of frequencies. The harmonic currents decrease as frequency increases, since at very high frequencies the criteria for large signal ($eV_{ac} >> \hbar\omega$) doesn't hold anymore. A frequency dependence of the admittance is only observed when the DB heterostructure is biased in the NDR region. Negative differential conductance gradually disappears as frequencies increase to the order of 10^{12} Hz (see Fig. 6). This characteristics will limit the maximum oscillation frequency of a DB heterostructure.

A parallel computation of transmission coefficients approach is first proposed to greatly increase the calculation speed of large-signal response of DB heterostructure in this paper. The degree of parallel computing is evaluated on Cray Y-MP8 supercomputer. In Table 1 we show that a speed-up around 45 and 70 can be reached with 64 and 128 processors parallel computer, respectively, when more than ten harmonics are used during the calculation.

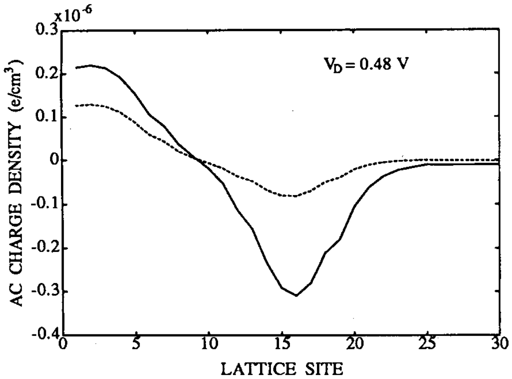

Fig.1 Initial (dashed) and final (solid) AC charge distribution.

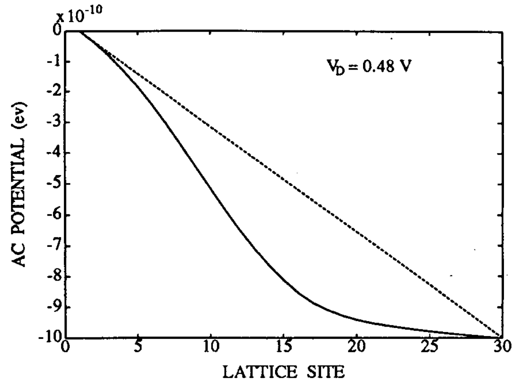

Fig.2 Initial (dashed) and final (solid) AC potential of structure I.

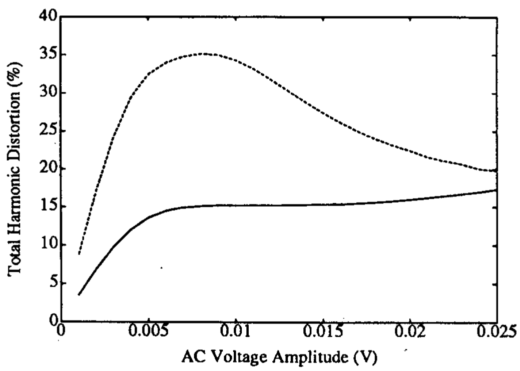

Fig.3 Total Harmonic distribution versus AC voltages.

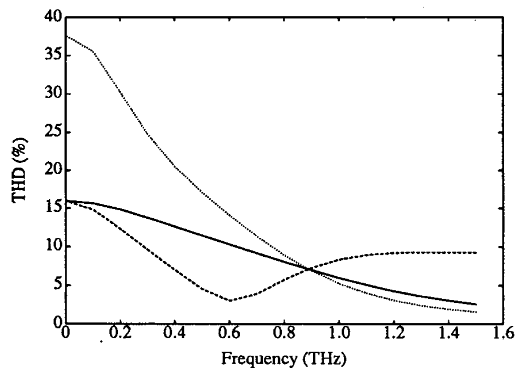

Fig.4 Total harmonic distribution as a function of frequency.

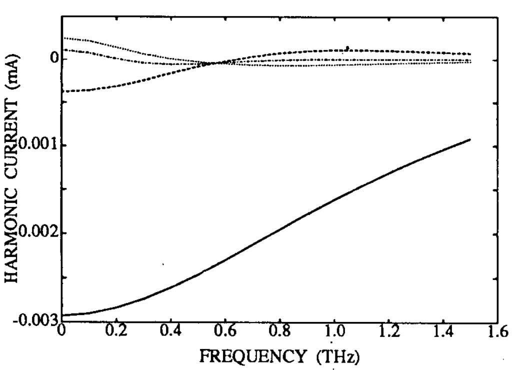

Fig.5(a) Frequency versus real part of harmonic current.

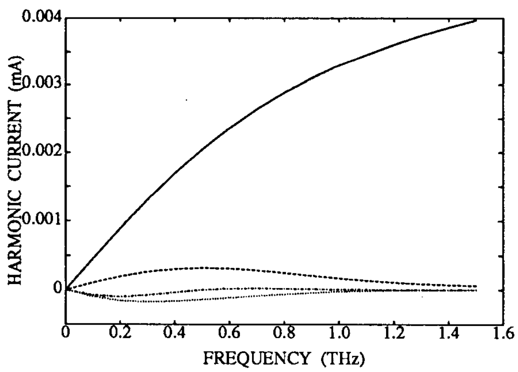

Fig.5(b) Frequency versus imaginary part of harmonic current.

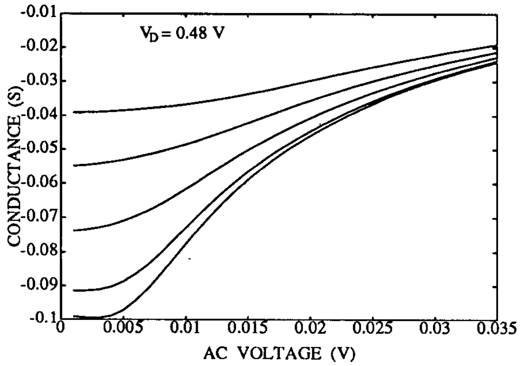

Fig.6 Amplitude variations of condcutance for several different frequency. (The frequency, starting from the top, are 1000, 750, 500, and 10GHz.)

Table 1: Speedup for different number of processors.

Number of Harmonic	Percentage of Parallel Parts	Speedup for 32 Processors	Speedup for 64 Processors	Speedup for 128 Processors
1	78.15	3.99	4.10	4.00
2	90.51	7.74	8.45	8.40
3	94.72	11.62	13.90	14.85
4	96.65	15.03	19.50	22.28
5	97.67	17.74	24.64	29.91
6	98.27	19.85	29.15	37.40
7	98.65	21.48	33.03	44.67
8	99.10	23.72	38.79	56.23
9	99.31	24.94	42.31	64.32
10	99.45	25.83	45.02	71.10